

## SMOS VEGETATION OPTICAL DEPTH AND ECOSYSTEM FUNCTIONAL PROPERTIES: EXPLORING THEIR RELATIONSHIPS IN TROPICAL FORESTS

*G. Vaglio Laurin (1), C. Vittucci (2), G. Tramontana (1), P. Bodesheim (3), P. Ferrazzoli (2), L. Guerriero (2), M. Jung (3), M. Mahecha (3), D. Papale (1)*

(1) Tuscia University, DIBAF, Viterbo, Italy

(2) Tor Vergata University, DICII, Rome, Italy

(3) Max Planck Institute for Biogeochemistry, Jena, Germany

### ABSTRACT

Data from the Soil Moisture and Ocean Salinity (SMOS) mission were recently exploited to derive ecosystem information. Here the strength of an innovative relationship, between SMOS V620 algorithm outputs and Ecosystem Functional Properties (EFPs) derived from flux towers data, was preliminary investigated for Africa and South America forests. High correlation values were found between SMOS vegetation optical depth (VOD) and EFPs, for the year under analysis (2014). The differences found at continental level and among different EFPs were commented, and related to the VOD sensitivity to above ground biomass. The results suggest that SMOS VOD data represent a tool able to provide repeated information on forest ecosystem processes and features at global scale.

**Index Terms** — Ecosystem Functional Properties, SMOS, Forests, Vegetation Optical Depth, Fluxnet

### 1. INTRODUCTION

The SMOS satellite, the second Earth Explorer Opportunity mission from the European Space Agency, carries on an L-band 2-D interferometric radiometer operating in the 1400–1427 MHz range. The dual polarization and multi-angular SMOS features are used to derive soil moisture and VOD from brightness temperature measurements [1]. Previous research [2–4] illustrated the sensitivity of VOD to forest attributes, such as forest height and above ground biomass, thanks to the volumetric scattering contribution that dominates in this land cover type. Similarly, VOD data from the Advanced Microwave Scanning Radiometer (AMSR-E) were used to produce global estimates of biomass for forest and non-forest biomes [5]. Thanks to sensitivity to forest properties and water content, and a high revisiting time, SMOS could be a useful instrument to provide information on carbon and water related forest ecosystem processes.

Indicators of forest ecosystem functional state, e.g. nutrient turnover, water cycling, and carbon storage potential, are fundamental to understand ecosystem processes, drivers of

change, and response to climate impacts. Ecosystem Functional Properties (EFPs) were recently defined by [6] “as quantities that characterize ecosystem processes and responses in an integrated and comparable manner”. EFPs characterize variations in key processes like photosynthesis, respiration, or evapotranspiration; or EFPs characterize the relationships among these processes, e.g. water use efficiency of photosynthesis, that represents the amount of carbon gained per water transpired. EFPs variability is partly due to environmental drivers and partly to biotic controls, such as plant abundance and traits [7,8]. EFPs can be derived by long-term point observations of gas and energy exchanges between the ecosystems and the atmosphere (e.g. flux towers data) by fitting response curves to light, temperature, and vapor-pressure deficit [9]. Remote sensing and gridded meteorological drivers, are used to upscale local measures using machine learning tools [6]. This upscaling process can introduce uncertainty, larger in regions -such as the tropical ones- where flux towers are scarce and availability of good quality satellite reflectance data is limited by cloud coverage. VOD data are not sensitive to cloud coverage and can potentially contribute to improve the upscaling process and reduce the uncertainty in the study of ecosystem processes at continental or global spatial scale. This preliminary analysis investigated the relations between SMOS VOD data and ecosystem functional state variables for pan-tropical forests: first, the link between VOD data and above ground biomass was evaluated, and then the relationships between VOD and EFPs derived by carbon and energy fluxes were analyzed.

### 2. MATERIALS AND METHODS

VOD values over Africa and South America, for the 2014 year, were obtained from V620 SMOS level 2 data, which are characterized by increased quality with respect to previous data versions. The VOD dataset was aggregated at monthly steps and spatially filtered to include only dense forested areas; considering SMOS 15 km spatial resolution a forest fractional coverage (FFO) > 90% was used to

minimize the inclusion of non-forested land. Then, VOD sensitivity to above ground biomass (AGB), as well as signal saturation, were evaluated using a biomass global map developed by [10] and resampled at VOD resolution. The relationship between VOD data and AGB map was tested at 25 Mg ha<sup>-1</sup> cumulated intervals, and the trend of the resulting coefficient of determination ( $R^2$ ) was used to find a threshold of AGB over which the VOD signal sensitivity saturates. Areas that in the AGB map showed values over this threshold were excluded from VOD dataset. A temporal filter was also used to select the period in which VOD showed more sensitivity to carbon related information, considering the influence of L-band signal of precipitation and the varying rainfall patterns along the year. A 3-month moving window (Jan.-Mar, Feb.-Apr, ... until Oct.-Dec.) was applied on the VOD dataset. The 3-month period for which the VOD-AGB map coefficient of determination resulted higher was used for the analyses.

The data used for generating the EFPs were provided by the Horizon 2020 BACI project (<https://www.bgc-jena.mpg.de/geodb/projects/Data.php>). These globally upscaled products, have been generated by a machine learning algorithm and site level half hourly measurements of carbon and energy fluxes provided by FLUXNET data (<http://fluxnet.fluxdata.org>). Products include Gross Primary Production (GPP) as carbon fluxes, Latent heat of evapotranspiration (LE) and sensible heat (H) among the energy fluxes. For calculating EFPs spatial grids of precipitation and global incoming radiation were also used. To explore correlations with SMOS VOD dataset, the following EFPs were used: maximum Gross Primary Production (GPPmax), Light Use Efficiency (LUE), Water Use Efficiency (WUE), and Bowen Ratio (BW). These EFPs provide empirical estimates of seasonal and long-term changes of ecosystem functional state and allow comparison across sites [7]. Specifically, GPPmax is an index of the photosynthetic capacity of the ecosystem, typically occurring at the peak of the growing season, with favorable temperatures and absence of water stress. GPPmax was estimated as the 90<sup>th</sup> percentile of daily GPP. LUE represents the capacity of vegetation to convert the incoming light to fixed carbon, and was calculated as the ratio between GPP and global incoming radiation (Rad). WUE, at ecosystem scale, is the capability of green ecosystem to optimize the available water that moves from soil to atmosphere through plant canopies; it was estimated as the ratio between GPP and evapotranspiration (derived by LE). BW is used to define the relative amount (as ratio) of energy used for warming in comparison with the one used for evapotranspiration; it was estimated as the ratio between H and LE. Additional details on EFPs products and processing are available at <https://www.bgc-jena.mpg.de/geodb/projects/Home.php> and illustrated by [7].

Upscaled fluxes and meteorological grids were processed to obtain EFPs for the 2014 year, and resampled to match the SMOS VOD spatial resolution. VOD-EFPs relationships were then explored by means of the Pearson and Spearman correlation coefficients.

### 3. RESULTS

#### 3.1 VOD and AGB map relationships

The VOD-AGB relationship for Africa and South America dense forests grew with increasing biomass and reached its maximum strength at about 275-300 Mg ha<sup>-1</sup> ( $R^2 = 0.68$ , 32766 samples), after which signal saturation occurred. The variability of the VOD-AGB map relationship according to different 3-month intervals is illustrated in Fig. 1. Results led to the selection of the Mar.-May and the Aug.-Oct. periods for Africa (17501 samples) and South America (36794 samples) respectively, being those in which VOD showed larger sensitivity to carbon related information.

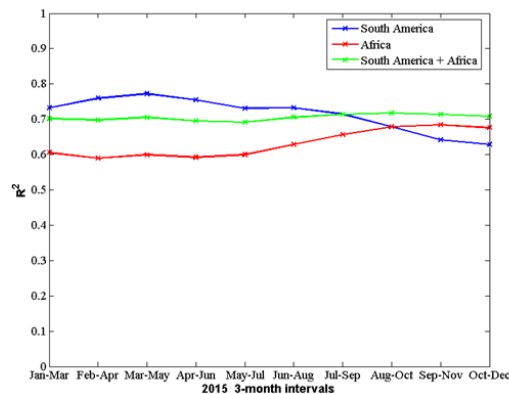


Figure 1.  $R^2$  trend for the VOD-AGB map relationship, in different 3-month intervals.

#### 3.2 VOD and EFPs relationships

Some of the computed EFPs are shown in Fig. 2 and 3, that illustrate GPPmax and LUE in South America, and in Fig. 4 and 5, that illustrate WUE and BW in Africa. These figures cover those areas retained after elimination of SMOS pixels with forest fraction lower than 90%. In Table 1, the Pearson and Spearman correlation coefficients computed between VOD (Mar.-May months in Africa and Aug.-Oct. in South America) and EFPs are presented.

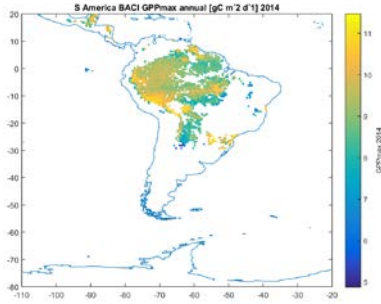


Figure 2. Map of GPPmax in South America.

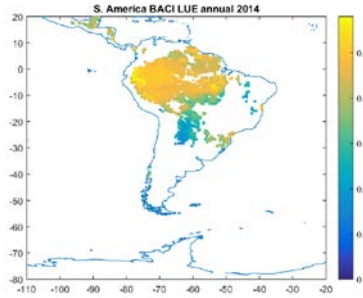


Figure 3. Map of LUE in South America.

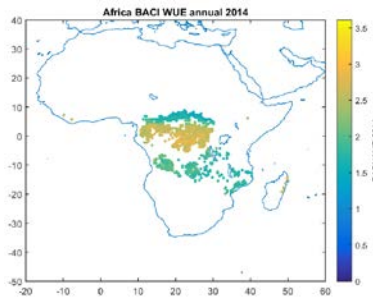


Figure 4. Map of WUE in Africa.

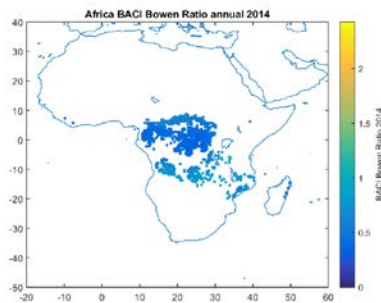


Figure 5 Map of BW in Africa.

Table 1. Values of Pearson and Spearman correlation coefficients between VOD and EFPs for the year 2014.

VOD	GPPmax	LUE	WUE	BW
Africa 2014 Spearman	0.78	0.83	0.81	-0.82
Africa 2014 Pearson	0.82	0.91	0.88	-0.86

S.America 2014 Spearman	0.22	0.60	0.54	-0.59
S.America 2014 Pearson	0.37	0.76	0.70	-0.67

Similarly, a correlation analysis was conducted between and EFPs and VOD monthly values; Fig. 6 shows VOD for the July 2015 month. The obtained results at monthly steps are in line with those obtained for year analysis; variations reflect the differences in meteorological patterns occurring in different regions along the year.

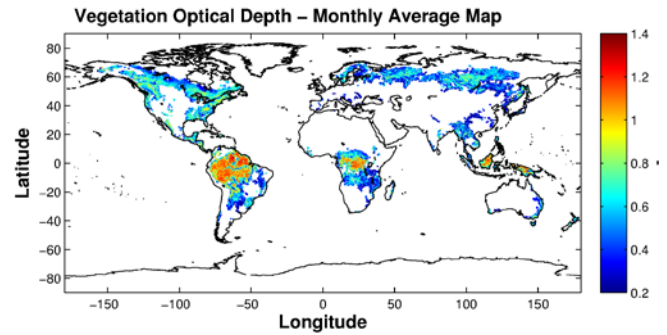


Figure 6. VOD averaged for the July month.

#### 4. DISCUSSION AND CONCLUSIONS

The relationship between VOD and AGB map resulted relevant, with signal saturation occurring at values that encompass most of the dense forests found in the tropical biome. This indicates that, at least in dense forests where the soil contribution to the signal is limited, SMOS data can provide important indications on the amount of stored carbon. When the 3-months VOD series were correlated to AGB, differences emerged between the two continents. The VOD-AGB correlation was in general slightly higher in South America, with minimal differences found along the year. The months in which the VOD-AGB correlation was higher were those having also higher precipitations regimes, in both continents: the Sept.-Dec. in the Congo Basin, and the Mar.-May period in the Amazon. During these months the VOD signal dynamic, and hence the correlation with AGB, resulted higher. It is known that the distribution of AGB density has a relation with water availability, at least in South America [11]. Rainfall can produce stronger VOD response in very dense forests with highest AGB, thanks to the water that remains captured in the canopy volume. In these forests the signal resulted high all along the year, as it probably reaches the saturation level. In less dense and open forests an increase of VOD is observed after the rainy season, due to regrowth, reducing the overall dynamic range. Therefore the highest dynamic range, as well as the highest correlation coefficient, are observed during the rainy

season. The correlations between EFPs and VOD were in general high, with the exception of the VOD-GPPmax relation, and better when tested with the Pearson coefficient with respect to the Spearman one, indicating linearity in the relationship. Pearson values resulted always higher for Africa than for South America; this might be caused by differences in VOD signal quality as well as in the uncertainty associated with EFPs in the two continents, with further studies needed to better assess the causes. For both continents, higher correlation was found between VOD and LUE and WUE, which are the two properties closely associated with carbon density. Anomalous lower correlation values were found between GPPmax and VOD in South America. This was partially explained exploring the regional values of the two datasets, as diverging patterns were found in areas outside the Amazonia core region, where GPPmax shows high values but VOD do not. These discrepancies are understandable when considering that vegetation productivity is not necessarily in line with AGB distribution, as shown for South America forests [12]. However, less clear and deserving further investigation is why this low VOD-GPPmax correlation did not occur for African forests. The future analysis, already on-going, will explore the relationships on multiple years, as well as for monthly series, and considering the variability in meteorological parameters. Overall, this preliminary study showed the potential of VOD to produce relevant information on Ecosystem Functional Properties, that can be exploited for improving their upscaling as well as to provide repeated information on ecosystem processes, related to water and carbon.

### Acknowledgements

This research was partially supported by the EU Horizon 2020 Research and Innovation Program under grant agreement 640176 and by ESA, European Space Agency.

## 5. REFERENCES

- [1] Y. H. Kerr, P. Waldteufel, P. Richaume, J.-P. Wigneron, P. Ferrazzoli, A. Mahmoodi, A. Al Bitar, F. Cabot, C. Gruhier, S. E. Juglea, D. Leroux, A. Mialon, S. Delwart, "The SMOS Soil Moisture Retrieval Algorithm", *IEEE Trans. Geosci. Remote Sensing*, vol. 50, pp. 1384–1403, 2012.
- [2] C. Vittucci, P. Ferrazzoli, Y. H. Kerr, P. Richaume, L. Guerriero, R. Rahmoune, G. Vaglio Laurin, "SMOS retrieval over forests: Exploitation of optical depth and tests of soil moisture estimates", *Remote Sensing of the Environment*, vol. 180, pp. 115–127, 2016.
- [3] Rahmoune, R., Ferrazzoli, P., Singh, Y. K., Kerr, Y. H., Richaume, P., & Al Bitar, A. SMOS retrieval results over forests: Comparisons with independent measurements. *IEEE Journal of Selected Topics in Applied Earth Observations and Remote Sensing*, 7, 3858–3866, 2014.
- [4] R. Rahmoune, P. Ferrazzoli, Y. H. Kerr, and P. Richaume, "SMOS level 2 retrieval algorithm over forests: Description and generation of global maps," *IEEE J. Sel. Topics Appl. Earth Observ. Remote Sens.*, vol. 6, no. 3, pp. 1430–1439, 2013.
- [5] Liu, Y. Y., Van Dijk, A. I., De Jeu, R. A., Canadell, J. G., McCabe, M. F., Evans, J. P., & Wang, G. Recent reversal in loss of global terrestrial biomass. *Nature Climate Change*, 5(5), 470–474, 2015.
- [6] Reichstein, M., Bahn, M., Mahecha, M.D., Kattge, J., Baldocchi, D.D., Linking plant and ecosystem functional biogeography. *Proc. Nat. Acad. Sci. U. S. A.* 111(38), 13697–13702, 2014.
- [7] Musavi, T., Mahecha, M. D., Migliavacca, M., Reichstein, M., van de Weg, M. J., van Bodegom, P. M., ... & Kattge, J. The imprint of plants on ecosystem functioning: A data-driven approach. *International Journal of Applied Earth Observation and Geoinformation*, 43, 119–131, 2015.
- [8] Musavi, T., Migliavacca, M., Reichstein, M., Kattge, J., Wirth, C., Black, T. A., ... & Varlagin, A. Stand age and species richness dampen interannual variation of ecosystem-level photosynthetic capacity. *Nature Ecology & Evolution*, 1, 0048, 2017.
- [9] Jung, M., Reichstein, M., Margolis, H. A., Cescatti, A., Richardson, A. D., Arain, M. A., ... & Gianelle, D. Global patterns of land-atmosphere fluxes of carbon dioxide, latent heat, and sensible heat derived from eddy covariance, satellite, and meteorological observations. *Journal of Geophysical Research: Biogeosciences*, 116(G3), 2011.
- [10] Avitabile, V., Herold, M., Heuvelink, G., Lewis, S. L., Phillips, O. L., Asner, G. P., ... & Berry, N. J. An integrated pan-tropical biomass map using multiple reference datasets. *Global change biology*, 22(4), 1406–1420, 2016.
- [11] Álvarez-Dávila, E., Cayuela, L., González-Caro, S., Aldana, A. M., Stevenson, P. R., Phillips, O., ... & Melo, O. Forest biomass density across large climate gradients in northern South America is related to water availability but not with temperature. *PloS one*, 12(3), e0171072, 2017.
- [12] Anderson, L. O. Biome-scale forest properties in Amazonia based on field and satellite observations. *Remote Sensing*, 4(5), 1245–1271, 2012.